Study of Nano structured SnO₂ activated MnO₂ Based LPG Sensors

R. R. Attarde[1], D. R. Patil[2]

[1]Department of physics, M. J. College, Jalgaon (MS) India
[2]Bulk and Nanomaterials Research Lab, Dept. of Physics, R. L. College, Parola (MS), India.

Abstract

The nano scaled material powder of MnO₂ was synthesized by Disc type ultrasonicated microwave assisted centrifuge technique. The characterizations and LPG gas sensing performance of pure and SnO₂ activated MnO₂ thick films have been investigated. Thick films of pure manganese oxide were prepared by screen printing technique. Pure manganese oxide was almost insensitive to LPG. However, SnO₂ activated MnO₂ thick films were observed to be most sensitive to LPG (15 min) at 300^0C. The efforts are made to develop the LPG gas sensor based on doping of pure MnO2 thick films. The quick response and fast recovery are the main features of this sensor. The effects of microstructure and additive concentration on the gas response, selectivity, response time and recovery time of the sensor in the presence of LPG gas were studied and discussed.

Keywords: SnO₂ activated MnO2, LPG gas sensor, Thick film, Low cost sensor.

1. Introduction

The conductometric semiconducting metal oxide gas sensors currently constitute one of the most investigated groups of gas sensors. They have attracted much attention in the field of gas sensing under atmospheric conditions due to their low cost and flexibility in production; simplicity of their use; large number of detectable gases/possible application fields. In addition to the conductivity change of gas-sensing material, the detection of this reaction can be performed by measuring the change of capacitance, work function, mass, optical characteristics or reaction energy released by the gas/solid interaction [1].

Numerous researchers have shown that the reversible interaction of the gas with the surface of the material is a characteristic of conductometric semiconducting metal oxide gas sensors [1]. This reaction can be influenced by many factors, including internal and external causes, such as natural properties of base materials, surface areas and microstructure of sensing layers, surface additives, temperature and humidity, *etc.* Many papers about metal oxide gas sensors have been published in recent years [1-20].

Over the past few decades, tin oxide based films are widely used as gas sensors due to their high sensitivity in the presence of small amounts of some gases of interest viz. carbon monoxide, ethanol, methane, LPG etc. Allied to this advantage is the simple design, robustness, fast response and the

possibility of miniaturization of these devices [21]. When a SnO_2 semiconductor film is exposed to air, physisorbed oxygen molecules receive electrons from the conduction band of the film and change to O^- ads or O^{2-} ads species. These adsorbed molecules form an electron depletion layer just below the surface of SnO_2 particles and forms a potential barrier between particles; consequently the SnO_2 film becomes highly resistive [22– 24]. The lowering of the potential barrier takes place when the adsorbed oxygen species are exposed to the reducing gases, resulting in the increased conductance of the sensitive film. The variation of the conductance measured under specific gases depends on many parameters such as intrinsic resistance, grain size [25], grain boundary barriers, detection temperature etc. Tin oxide films have been prepared by a number of techniques including spray pyrolysis [26, 27], sputtering [28, 29], chemical vapour deposition (CVD) [30] and evaporation [31].

In this investigation, a synthesis procedure was developed to obtain tailored nano particle films from dipping of tin oxide nano particles into MnO_2. Various particle and film characteristics can be independently controlled for LPG gas sensor.

2. Experimental procedure

2.1 Synthesis of nanostructured MnO_2 powder

The nanostructured MnO_2 and SnO_2 doped MnO_2 powders were synthesized by the hydrolysis of AR grade manganese chloride (99.9 % pure) in aqueous-alcohol solution. An initial aqueous-alcohol solution was prepared from distilled water and propylene glycol. Then the hydroxide in a glass beaker was placed in a microwave oven (input power 600W) for 15 minutes with on-off cycle. The dried precipitate was ground by using agate pestle mortar and annealed in a muffle furnace at 550°C for 30 min. The phase purity and the degree of crystallinity of the resulting MnO_2 powder were monitored by XRD analysis.

2.2 Thick films Fabrication

The fine powders of MnO_2 and SnO_2 dipped MnO_2 were calcinated at 800^0C for 24 h in air and reground to ensure sufficiently fine particle size. The thixotropic paste was formulated by mixing the synthesized nanostructured powders of pure and doped MnO_2 (one at a time) with a solution of ethyl cellulose (a temporary binder) in a mixture of organic solvents such as butyl cellulose, butyl carbitol acetate and turpineol. The ratio of inorganic to organic part was kept as 80: 20 in formulating the paste. The thixotropic paste was screen printed on the glass substrate in desired patterns. Films prepared were fired at 550^oC for 30 min in ambient air.

2.3 Surface activation of thick films

Surface activation of thick films of pure MnO_2 powder was achieved by dipping them into a 0.01 M aqueous solution of tin chloride for different intervals of time such as 15 min, 30 min, 45 min and 60 min. and was dried at 70-120 ^{o}C under an IR lamp, followed by firing at 550°C for 30 min in ambient air. The particles of tin chloride dispersed on the film surface would be transformed to tin oxide (SnO_2) during firing process. Thus, the sensor elements with different dipping time of SnO_2 incorporated in to thick films were prepared. Silver contacts were made by vacuum evaporation for electrical measurements and monitoring the gas sensing performance of thick films

3. Materials characterization

3.1 Micro structural analysis

3.1.1 Unmodified (Pure) MnO_2

Figure 1 shows SEM images of MnO_2 thick film with magnification 120K. The SEM image of MnO_2 thick film show that the film is uniform, polycrystalline, well cover on glass slide and free from microscopy defect like cracks or peeling. The films consist of some voids which can be used for doping of another material to improve the structure. Nano size grains were uniformly distributed over smooth homogeneous background. The particle sizes were found to be 40 – 80 nm.

S-4800 15.0kV 8.3mm x120k SE(U) 21/02/2015 14:40   400nm
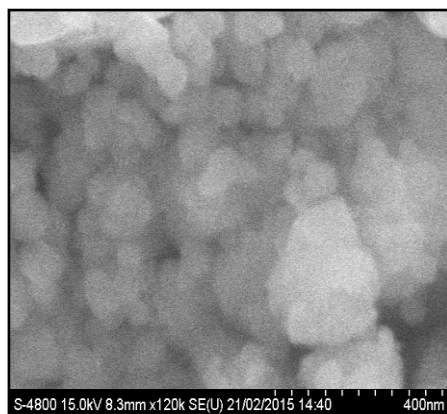
Fig. 1: Micrograph of unmodified MnO_2 film

3.1.2 SnO_2 activated MnO_2

A Monthly Double-Blind Peer Reviewed Refereed Open Access International e-Journal - Included in the International Serial Directories

International Journal in Physical & Applied Sciences

http://www.ijmr.net.in email id- irjmss@gmail.com   Page 23
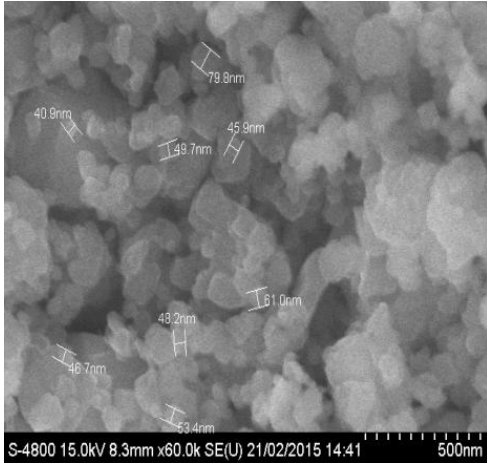
Fig. 2 (a) Micrograph of SnO$_2$ activated MnO$_2$ (15')
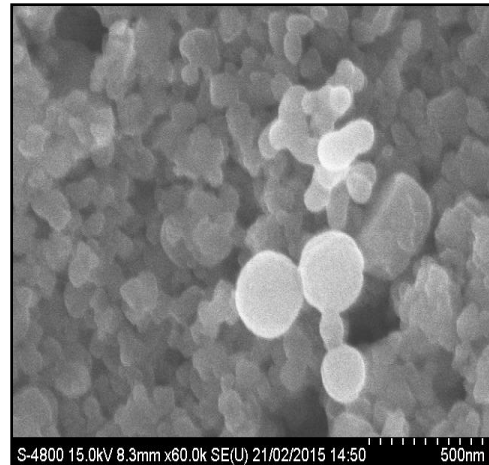
Fig. 2 (d) Micrograph of SnO$_2$ activated MnO$_2$ (60')
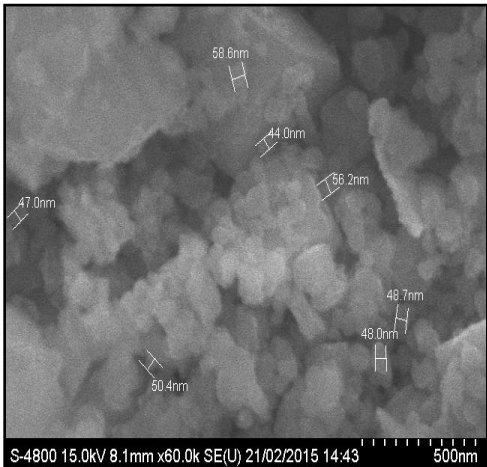
Fig. 2 (b) Micrograph of SnO$_2$activated MnO$_2$ (30')
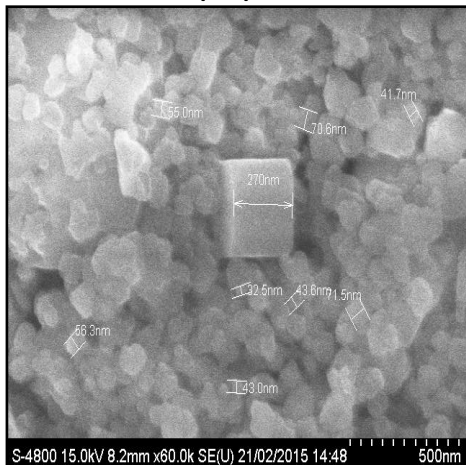
Fig. 2 (c) Micrograph of SnO$_2$ activated MnO$_2$ (45')

Fig. 2 (a - d) depicts the microstructures of SnO_2-activated MnO_2 thick films consisting of number of particles of Sn-species distributed on the MnO_2 surface. Figure shows that a few grains of MnO_2 in the film are masked with a very thin layer of Sn-species. This film was observed to be the most sensitive film. The masking of the films increases with dipping time. The entire masking of the films in sufficient proportion resists the gas to reach the active sites of the surface of the film. This would decrease the gas sensing performance of the films at higher dipping time (i. e. > 30 min). It is clear from figures that with the increase of dipping time interval, there is a change in the surface texture of the films. Larger the dipping time interval, larger would be the amount of SnO_2 dispersed on the surface, and smaller would be the chances of reaching the gas to base material. The dipping time interval was, therefore, optimized to have optimum number of SnO_2 misfits dispersed uniformly on the surface so as to contribute effective enhancement of gas sensing.

3.1.3 Elemental Analysis (EDAX)

The quantitative elemental composition of pure and SnO_2-activated MnO_2 thick films were analyzed using an energy dispersive spectrometer in the binding energy region between 0 to 10 KeV and found the mass % of Sn, O, SnO_2, Mn and MnO_2. Stoichiometrically expected % mass of Mn and O_2 (in MnO_2) are 87.98 and 12.02 respectively.

Pure stoichiometric MnO_2 is expected to be insulating. Stoichiometrically expected mass % of Mn and O (in MnO_2) are 63.19 and 36.81, respectively. The analysis showed that, the mass % of Mn and O in each samples are not as per the stoichiometric proportion and all samples are observed to be the oxygen deficient. Also, the films dipped in 0.01 M aqueous solution of tin chloride were observed to be most oxygen deficient than the pure films. Excess or deficiency of the constituent material particles leads the semiconducting nature of the material.

It is clear that the unmodified MnO_2 is more oxygen deficient and oxygen deficiency could be reduced by adding SnO_2 into MnO_2. The mass % of SnO_2 goes on increasing with the dipping time, reaches to a maximum and then decreases with a further increase in dipping time. This could be attributed to the dispersion and intrusion of Sn grains on the surface of the film. The SnO_2 mass % (1.44) is highest for a 30 min dipping time. Due to an increase in mass % of Sn there was a decrease in the mass % of Mn.

3.2 Electrical properties

3.2.1 I-V characteristics

Fig. 3 (a, b) represents I-V characteristics of the SnO_2 dipped MnO_2 films at room temperature and at high temperature. It is clear from the symmetrical I-V characteristics that the contacts fabricated on the films were ohmic in nature and the p-n junctions were randomly distributed on the surface of the film. The material is therefore said to have resistive properties

A Monthly Double-Blind Peer Reviewed Refereed Open Access International e-Journal - Included in the International Serial Directories

International Journal in Physical & Applied Sciences

http://www.ijmr.net.in email id- irjmss@gmail.com   Page 25

(a)   (b)
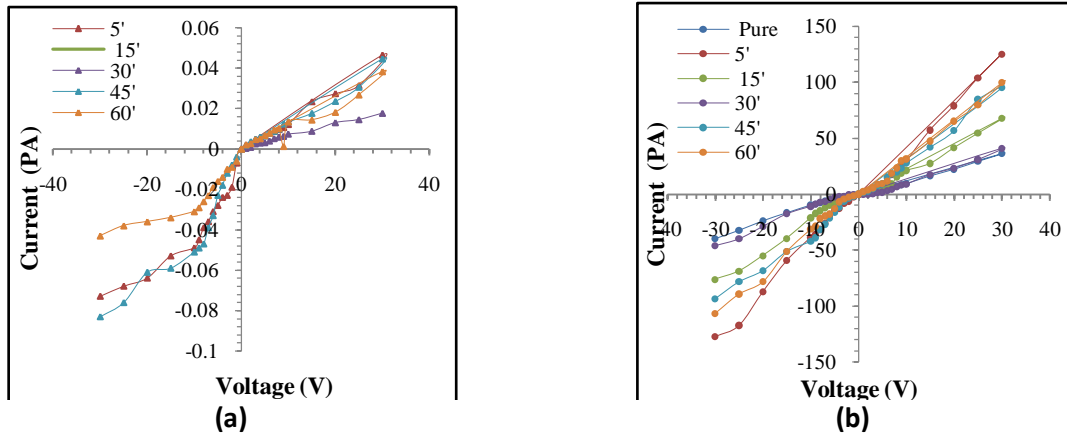
Fig. 3 (a, b) I-V characteristics of sensor at RT and at High Temperature

3.2.2 Electrical conductivity
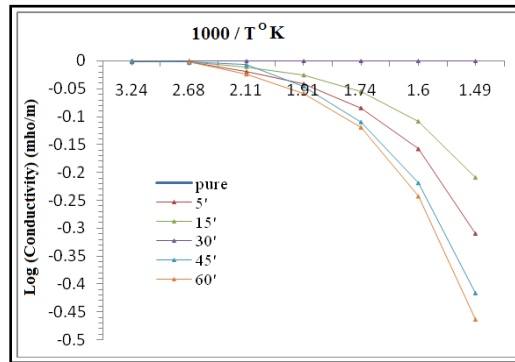
Fig. 4: Conductivity-temperature profile of SnO$_2$ activated MnO$_2$ films

Fig. 4 depicts the variation of log (conductivity) with operating temperature of pure and SnO$_2$ activated MnO$_2$ thick films. The semiconducting nature of MnO$_2$ is observed from the measurement of conductivity with temperature. The conductivity values of all samples were larger at room temperature than at higher temperature. It may be due to air humidity associated with the films at room temperature. The increase in conductivity with increasing temperature (above 100^{0}C) could be attributed to negative temperature coefficient and semiconducting nature of the SnO$_2$ activated MnO$_2$ samples. The SnO$_2$ activated films showed very high electrical resistance of the order of 10^7 Ω in air.

From figure, it is clear that the conductivity of the sensor increases with decrease in operating temperature, indicating a positive temperature coefficient of resistance. This behavior confirmed the semiconducting nature of the undoped and activated MnO$_2$.

3.3 Gas sensing properties

3.3.1 Effect of operating temperature

Fig. 5 shows the variation of LPG vapors (300 ppm) response of pure MnO$_2$ with operating temperature. The lowest and random response for LPG gas was observed as a function of operating temperature. The maximum response obtained is of the order of 95 at 50^{0}C. The response curve

shows the random increase and decrease with respect to temperature. So, it is the need to modify the bulk and / or surface of the base material to enhance the gas sensing performance and its selective nature to a particular gas among the mixture of various gases.
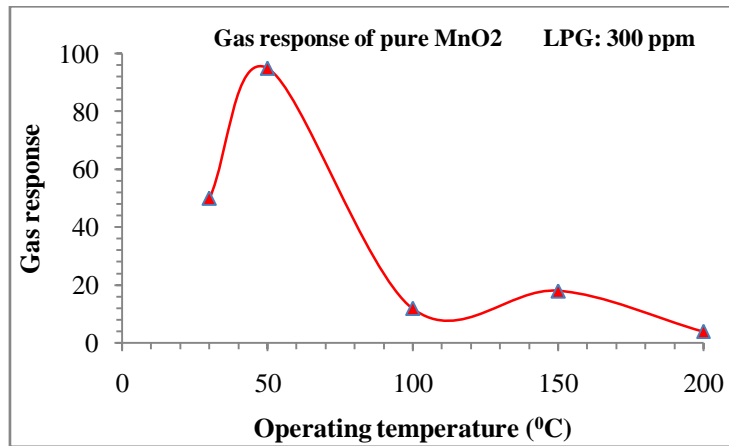
Fig. 5 Variation of gas responses of pure MnO$_2$ thick film with temperature

3.3.2 Selectivity
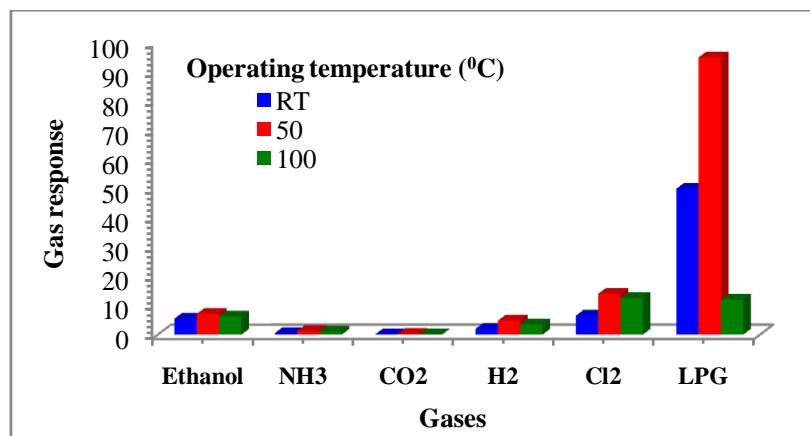
Fig. 6 Selectivity of pure MnO$_2$

It is observed from Fig. 6 that the pure MnO$_2$ is sensitive to LPG gas at 50°C. However, it has least selectivity to LPG gas against different gases viz. ethanol, ammonia and carbon dioxide. This is the major drawback of pure MnO$_2$ thick films. So, it is the today's need to modify the pure MnO$_2$.

3.3.3 SnO$_2$-Activated MnO$_2$ films

3.3.3.1 Effect of operating temperature
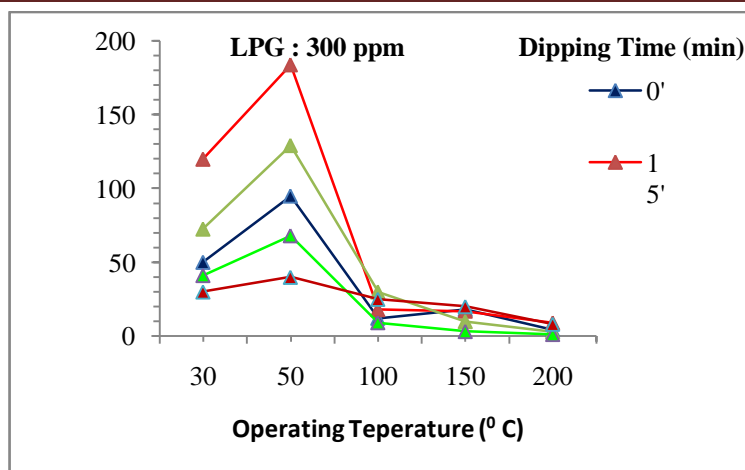
Fig. 7 Variation of gas response with operating temperature (^{o}C)

The response of SnO_2 - modified MnO_2 films to 300 ppm LPG, as a function of operating temperature is shown in Fig. 8. From the figure, it is observed that the gas response increases with operating temperature, reaches maximum at 50^0C and decreases with further increase in temperature. The MnO_2 - modified MnO_2 (15 min, 1.04 mass % SnO_2) It is clear from figure that the LPG response of SnO_2-activated MnO_2 (15') thick film increases with operating temperature, reaches to maximum (184) at 50^0C, and falls with further increase in operating temperature. The LPG may burn before reaching the surface of the film at higher temperature (> 50^0C). Hence, the gas response may decrease above 50^0C.

3.3.3.2 Active region of the sensor
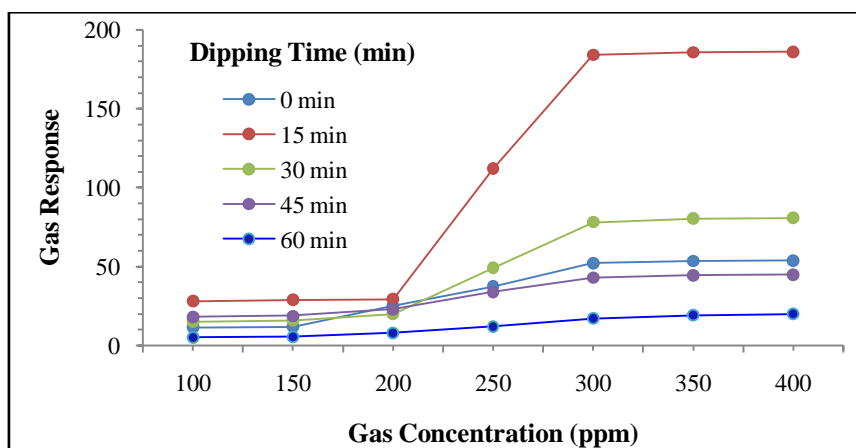
Fig. 8 Variation in response with LPG vapor concentration (ppm)

It is clear from the Fig. 8 that the LPG response of SnO_2-activated MnO_2 increases linearly, attains the maximum and saturates above 300 ppm gas at 50^0C. The variation of gas response of SnO_2 activated MnO_2 (15 min) sample with LPG vapor concentration (ppm) at 50^0C is represented in Figure. This film was exposed to varying concentrations of LPG vapors. For the SnO_2 activated MnO_2 samples, the response values were observed to increase linearly with increasing gas concentration up to 300 ppm at 50^0C. The rate of increase in LPG response was relatively larger up to 300 ppm,

smaller above 300 ppm and saturated beyond it. Thus, the active region of the sensor would be up to 300 ppm. For proper functioning of the sensors, the best region to operate is the only active region.

The excess gas would form saturated environment on the sensor surface and a part of gas amount would be unable to reach and interact with active sites of the sensor material. Hence response would not increase further.

3.3.3.3 Effect of dipping time

Fig. 9 depicts the variation of gas response to LPG with dipping time respectively. The sample, activated for 15 min in 0.01 M tin chloride was observed to be the most sensitive to LPG vapors among all at 50^oC.
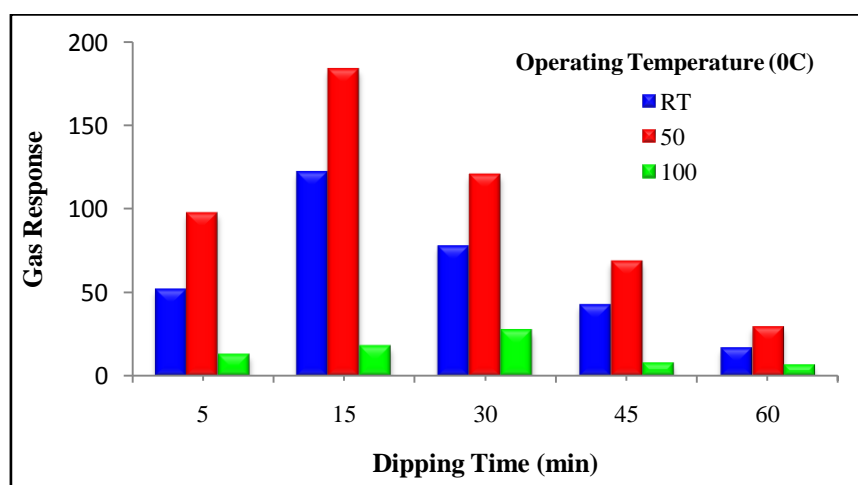
Fig. 9 Variation of LPG response with dipping time

It showed the highest response to 300 ppm LPG vapors at 50^0C. The highest response of this sample as compared to other SnO_2 activated samples may be due to the optimum number of SnO_2 grains dispersed on the surface which enhance the adsorption and oxidation of LPG vapors quickly. It is observed that the gas response is largest at optimum mass % of SnO_2. At higher mass %, the Sn-surfactant would mask the base material (MnO_2) and resist the gas to reach to the surface sites, so that the gas response would decrease.

3.3.3.4 Selectivity

Fig. 10 depicts the selectivity of the sensor to LPG vapors at 50^0C. The activated sensor (15') showed high selectivity for LPG and could distinguish trace level of LPG (300 ppm) among all the gases viz: NH_3, CO_2, ethanol, H_2, Cl_2, H_2S, etc. even at higher concentrations (1000 ppm).

A Monthly Double-Blind Peer Reviewed Refereed Open Access International e-Journal - Included in the International Serial Directories

International Journal in Physical & Applied Sciences

http://www.ijmr.net.in email id- irjmss@gmail.com   Page 29

	C12	NH3	CO2	C2H5OH	H2	LPG
■ 5'	16	3.25	1.27	9.1	6.8	52
■ 15'	22.3	3.34	5.75	13.3	7.5	122
■ 30'	38.2	3.86	9.76	27.8	8.41	78
■ 45'	27.4	4.21	7.08	9.43	8.98	43
■ 60'	19.3	4.67	4.45	8.6	7.91	17

Fig. 10: Selectivity of LPG vapors from the mixture of gases

3.3.3.5 Response and recovery time
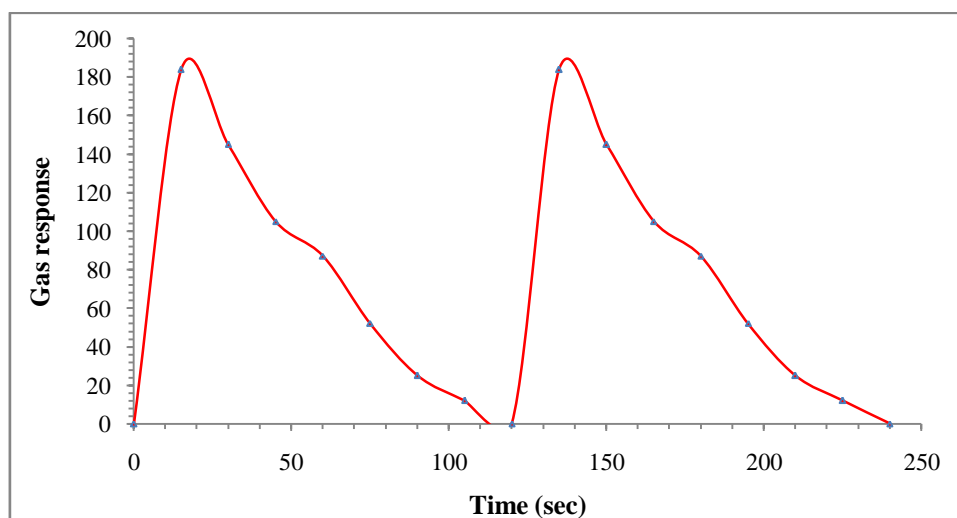
Fig. 11: Response and recovery of SnO$_2$ activated MnO$_2$ sample

The response and recovery of the SnO$_2$ activated MnO$_2$ (SnO$_2$: MnO$_2$ = 1.04: 1) sensors are represented in Fig. 11. The response was quick (~ 15 s) to 300 ppm of LPG, while the recovery was fast (~ 105 s). The fast response may be due to immediate oxidation of LPG gas. The negligible quantity of the surface reaction product and its high volatility explains its fast response to LPG and quick recovery to its initial chemical status.

Summary Table

Samples	Gas sensing performance					Optimum operating conditions		
	Max. Sensing gas	Gas response	Gas conc. (ppm)	Response time (s)	Recovery time (s)	Op. temp. (^{0}C)	Dop. Conc. (wt.%)	Dip. Time (min)
Pure MnO$_2$	LPG	17	300	15	105	50^{0}C	--	--
SnO$_2$ - activated MnO$_2$	LPG	122	300	15	105	50^{0}C	--	15'

3.4. Discussion: Mechanisms for Gas Sensing in SnO₂

Sensors with Additives Decreasing the SnO_2 crystallite size can dramatically improve sensor sensitivity; however, the small dimensions required are difficult to achieve in a practical sensor. Additives can have several effects on the SnO_2 properties important to gas sensing applications, including inhibiting MnO_2 grain growth, modifying the electron Debye length and modifying the gas-surface interactions. Heat treatment processes are integral to sensor fabrication, and these processes result in significant restructuring of the MnO_2 crystallites. Additives can limit the extent of the SnO_2 coalescence. Additives can also change the gas-surface interactions of a tin oxide sensor. As the butane [32] is the major constituent of LPG, it requires high temperature to dissociate into lower alkanes. Carbon-carbon and carbon-hydrogen bonds are quite strong due to strong Vander Waals forces. They break only at higher temperatures resulting in carbon and hydrogen separation. The atmospheric oxygen O_2 adsorbs on the surface of the thick film. It captures the electrons from conduction band as:

$$O_{2\,(air)} + 4e^- \rightarrow 2O^{2-}_{(film\ surface)}$$
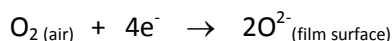
It would result in decreasing conductivity of the film.

When alkanes react with oxygen, a complex series of reactions [30 -32] take place, ultimately converting the alkanes to carbon dioxide and water as:

$$CH_{4\,(gas)} + 4\,O^{2-}_{(film\ surface)} \rightarrow CO_{2\,(gas)} + 2\,H_2O_{(gas)} + 8\,e^-_{(cond.\ band)}$$

$$C_2H_{6\,(gas)} + 7\,O^{2-}_{(film\ surface)} \rightarrow 2\,CO_{2\,(gas)} + 3\,H_2O_{(gas)} + 14\,e^-_{(cond.\ band)}$$

$$C_3H_{8\,(gas)} + 10\,O^{2-}_{(film\ surface)} \rightarrow 3\,CO_{2\,(gas)} + 4\,H_2O_{(gas)} + 20\,e^-_{(cond.\ band)}$$

$$C_4H_{10\,(gas)} + 13\,O^{2-}_{(film\ surface)} \rightarrow 4\,CO_{2\,(gas)} + 5\,H_2O_{(gas)} + 26\,e^-_{(cond.\ band)}$$
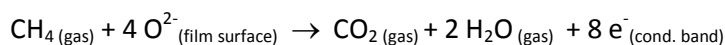
This shows n-type conduction mechanism. At higher temperature, molecular oxygen O_2 becomes O_2^- and alkanes decompose producing hydrogen ions H^+ in the reaction. The anion super-oxide O_2^- reacts with H^+ giving water molecule and molecular oxygen O_2:

$$2O_2^- + 2\,H^+ \rightarrow H_2O_2 + O_2$$

Catalase

$$2\,H_2O_2 \rightarrow 2\,H_2O + O_2$$
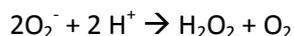
LPG gas on exposure decomposes into carbon and hydrogen species which react with adsorbed oxygen, liberating the captured electrons into conduction band resulting in enhancing the catalytic activity of the film surface. The rate of adsorption and the reaction between the adsorbed species depends, of course, on temperature. Gas response versus operating temperature curves of semiconductor gas sensors usually shows a maximum at certain temperature which is used as the working temperature of that sensor.
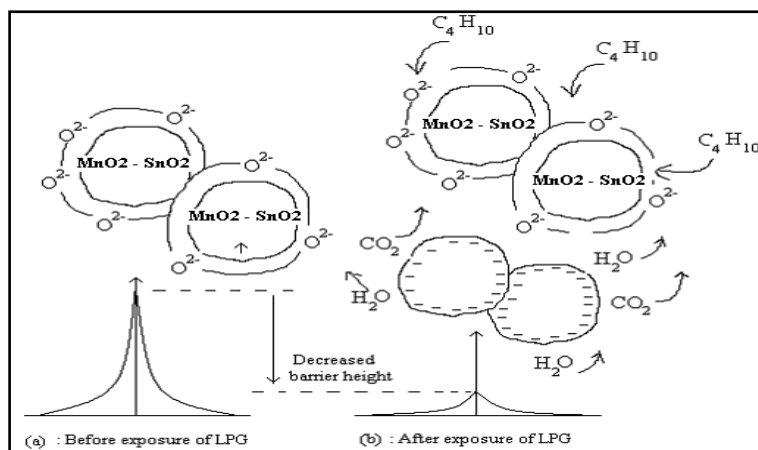
Fig. 12: LPG gas sensing mechanism of MnO_2 – SnO_2 films

In addition to the effect of temperature on the kinetics of the reaction between the adsorbed species, findings on MnO_2 sensors reveal another effect of temperature on sensing. It was observed that, as the temperature was changed, the form of the adsorbed oxygen was also changed. Therefore, the generally observed shape of the gas response curve is also affected by the changes in the nature and coverage of adsorbed oxygen as a function of temperature. This temperature which shows the maximum response can be used as a means of selectivity between reducing gases having maxima at different temperatures. If a surface additive that specifically adsorbs or reacts with the gas of interest is used, then this can increase selectivity.

4. Conclusions

From the results, following statements can be made for the sensing performance of the present SnO_2-modified sensors.

1. Pure MnO_2 was poor sensitive to LPG gases at higher temperatures.

2. Pure MnO_2 showed gas response, though small, to LPG at high operating temperature.

3. Among various additives tested, SnO_2 was observed to be outstanding in promoting the gas sensing performance of MnO_2 based gas sensors.

4. Surface modification by dipping process was one of the most suitable methods of modifying the thick film surface.

5. A modified film with 1.04 mass % of SnO_2 in MnO_2 was observed to be the most sensitive element to LPG gas.

6. SnO_2-modified MnO_2 has the potential of fabricating a room temperature LPG sensor.

7. The sensor showed very rapid response and recovery.

5. References

1. Korotcenkov, G. *Mater. Sci. Eng. B* 139 (2007) 1-23.

2. Barsan, N., Koziej, D., Weimar, U. *Sens. Actuat. B* 121 (2007) 18-35.

3. Korotcenkov, G. *Mater. Sci. Eng. R* 61 (2008) 1-39.

4. Batzill, M. *Sensors* 6 (2006) 1345- 1366.

5. Barsan, N.; Schweizer-Berberich, M.; Göpel, W. Fresenius *J. Anal. Chem.* 365 (1999) 287-304.

6. Park, C.O.; Akbar, S.A. *J. Mater. Sci.* 38 (2003) 4611-4637.

7. Batzill, M.; Diebold, U. *Prog. Surf. Sci.* 79 (2005) 47-154.

8. Moos, R.; Sahner, K.; Fleischer, M.; Guth, U.; Barsan, N.; Weimar, U. *Sensors* 9 (2009) 4323-4365

9. Rumyantseva, M.N.; Gas'kov, A.M. *Russ. Chem. Bull.* 57 (2008) 1106-1125.

10. Lee, J.H. *Sens. Actuat. B* 140 (2009) 319-336.

11. Fergus, J.W. *Sens. Actuat. B* 123 (2007) 1169-1179.

12. Lu, J.G.; Chang, P.C.; Fan, Z.Y. *Mater. Sci. Eng. R* 52 (2006) 49-91.

13. Orton, J.W.; Powell, M.J. *Rep. Prog. Phys.* 43 (1980) 1263-1307.

14. Rothschild, A.; Komem, Y. *J. Electroceram.* 13 (2004) 697-701.

15. Rothschild, A.; Komem, Y. *J. Appl. Phys.* 95 (2004) 6374-6380.

16. Comini, E.; Baratto, C.; Faglia, G.; Ferroni, M.; Vomiero, A.; Sberveglieri, G. *Prog.Mater. Sci.* 54 (2009) 1-67.

17. Korotcenkov, G. *Sens. Actuat. B* 107 (2005) 209-232.

18. Yamazoe, N.; Shimanoe, K. *Sens. Actuat. B* 138 (2009) 100-107.

19. Tiemann, M. *Chem. Eur. J.* 2007, *13*, 8376-8388.

20. Eranna, G.; Joshi, B.C.; Runthala, D.P.; Gupta, R.P. *Crit. Rev. Solid State Mater. Sci.* 29 (2004) 111-188.

21. Dutaive M S, Lalauze R and Pijolat C Sensors & Actuators B26 (1995) 27 38.

22. Coutts T J, Pearsall N M and Tarricane L; J. Vac. Sci. Technol. B2 (1984) 140.

23. Coutts T J, Li X and Cessert T A; IEEE Electron Lett. 26 (1990) 660.

24. Gardener J W, Shurmer H V and Corcoran P, Sensors & Actuators B4 (1991) 117.

25. Lalweze R and Pizolat C; Sensors & Actuators 5 (1984)55.

26. Tarey R D and Raju T A; Thin Solid Films 221 (1985) 181.

27. Lane D W, Coath J A and Beldon H S; Thin Solid Films 221 (1992) 262.

28. Karasawa T and Miyata Y Thin Solid Films 223 (1993) 135.

29. Kulkarni A K and Knickerbocker S A Thin Solid Films 220 (1992) 321.

30. Park S S, Zheng H and Mackenzie J D Thin Solid Films 258 (1995) 268.

31. Brinker C J, Hurd A J, Schunk P R, Frye G C and Ashley C S J. Non-Cryst. Solids 424 (1990) 147.

32. Z. Tianshu, Z. Ruifang, S. Yusheng, L. Xingqin, Sens. Actuators, B 32 (1996) 185-189.

A Monthly Double-Blind Peer Reviewed Refereed Open Access International e-Journal - Included in the International Serial Directories

International Journal in Physical & Applied Sciences

http://www.ijmr.net.in email id- irjmss@gmail.com   Page 33